

First lattice study of low-energy charmonium-hadron interaction

Kazuo Yokokawa⁽¹⁾, Shoichi Sasaki^(1,2), Tetsuo Hatsuda⁽¹⁾ and Arata Hayashigaki⁽³⁾

⁽¹⁾ Department of Physics, The University of Tokyo, Tokyo 113-0033, Japan

⁽²⁾ RIKEN BNL Research Center, Brookhaven National Laboratory, NY 11973, USA and

⁽³⁾ Institut für Theoretische Physik, J.W. Goethe Universität, D-60438 Frankfurt, Germany

(Dated: May 25, 2019)

We study the scattering lengths of charmonia (J/ψ and η_c) with light hadrons (π , ρ and N) by the quenched lattice QCD simulations on $24^3 \times 48$, $32^3 \times 48$ and $48^3 \times 48$ lattices with the lattice spacing $a \simeq 0.068$ fm. The scattering length is extracted by using the Lüscher's phase-shift formula together with the measurement of the energy shift ΔE of two hadrons on the lattice. We find that there exist attractive interactions in all channels, $J/\psi(\eta_c)\text{-}\pi$, $J/\psi(\eta_c)\text{-}\rho$ and $J/\psi(\eta_c)\text{-}N$: The s -wave $J/\psi\text{-}\pi$ ($\eta_c\text{-}\pi$) scattering length is determined as 0.0119 ± 0.0039 fm (0.0113 ± 0.0035 fm) and the corresponding elastic cross section at the threshold becomes $0.018^{+0.013}_{-0.010}$ mb ($0.016^{+0.011}_{-0.008}$ mb). Also, the $J/\psi\text{-}N$ ($\eta_c\text{-}N$) spin-averaged scattering length is 0.71 ± 0.48 fm (0.70 ± 0.66 fm), which is at least an order of magnitude larger than the charmonium-pion scattering length. The volume dependence of the energy shifts is also investigated to check the expected $1/L^3$ behavior of ΔE at a large spatial size L .

PACS numbers: 11.15.Ha, 12.38.-t 12.38.Gc

I. INTRODUCTION

Properties of single hadrons have been studied in quantum chromodynamics (QCD) by using various techniques such as the QCD sum rules and lattice QCD simulations. On the other hand, the interaction between color-singlet hadrons is not fully explored yet because of their complex nature originating from quark exchanges and multiple gluon exchanges.

In this paper, we study the low-energy elastic scattering of charmonia (J/ψ and η_c) with iso-nonsinglet hadrons composed of up and down quarks (π , ρ and N) on the basis of the quenched lattice QCD simulations. Since the valence quarks in each hadron in the initial state stay in the same hadron in the final state, the process we consider is much simpler than the interactions between light-hadrons, while it is still non-trivial in the sense that non-perturbative gluon exchanges play essential roles. Furthermore, such interaction has a direct relation to the physics of charmonium-nucleus (A) bound states [1, 2, 3, 4, 5] and an indirect relation to the the elastic and inelastic charmonium-hadron interactions at high energies [6, 7, 8].

The charmonium- N interaction at low energies has been discussed in the framework of operator product expansion [9, 10, 11, 12, 13, 14] and in some hadronic model [8]. For example, Hayashigaki has shown that the s -wave $J/\psi\text{-}N$ scattering length $a_0^{J/\psi\text{-}N}$ is about 0.1 fm by using QCD sum rules [12], while Brodsky and Miller found that it is about 0.25 fm from the gluonic van der Waals interaction [4]. Recently, Sibirtsev and Voloshin suggested that a lower bound of the $a_0^{J/\psi\text{-}N}$ is as large as 0.37 fm from the multipole expansion analysis of chromo-polarizability [13]. In the above-mentioned calculations, the elastic cross section at the threshold reads 1.3 mb, 7.9 mb and 17 mb, respectively. Brodsky, Schmidt and de Téramond introduced an effective charmonium-nucleon potential $V(r) = -\alpha e^{-\mu r}/r$ with the parameters $\alpha = 0.42 \sim 0.59$ and $\mu = 6.0$ GeV estimated by a phenomenological model of Pomeron interactions [1]. They argued that the $J/\psi\text{-}A$ bound system may be realized for mass number $A \geq 3$ if the attraction is sufficiently large, which was later confirmed by Wasson, who solved the Schrödinger equation for the charmonium-nucleus system [2].

Unlike the case of $J/\psi\text{-}N$, the interaction of the charmonium with the pion has a special feature due to the Nambu-Goldstone nature of the pion. The current algebra shows that the s -wave scattering length of a heavy hadron (H) with the pion is given by the well-known formula [15]:

$$a_0^{H\text{-}\pi} = - \left(1 + \frac{M_\pi}{M_H} \right)^{-1} \frac{M_\pi}{4\pi f_\pi^2} \vec{I}_\pi \cdot \vec{I}_H + O(M_\pi^2), \quad (1)$$

where \vec{I}_π (\vec{I}_H) is the isospin vector of π (H) and $\vec{I}_\pi \cdot \vec{I}_H = \frac{1}{2} [I(I+1) - I_H(I_H+1) - 2]$ with I being the total isospin of the $\pi\text{-}H$ system. For the $\pi\text{-}N$ case, this is known as the Tomozawa-Weinberg relation. Eq. (1) indicates that the soft pion decouples from any hadrons in the chiral limit ($M_\pi \rightarrow 0$). More importantly in our context, the leading term in Eq. (1) vanishes even if M_π is finite as long as H is iso-scalar (such as J/ψ and η_c): Namely, the low-energy pion interaction with the charmonium states is very weak of $O(M_\pi^2)$. An alternative estimate based on the color-dipole description of heavy quarkonia shows a small but attractive interaction between the charmonium and

the pion [10, 11, 16]. Here, the contribution stems from the QCD trace anomaly and the effect starts from $O(M_\pi^2)$ as consistent with the current algebra analysis [17].

The method we employ for extracting the charmonium-hadron scattering lengths is the quenched lattice QCD simulations together with the phase-shift formula by Lüscher [18]. The basic idea is to put two hadrons in a finite box with a spatial size L and to measure the energy of interacting hadrons relative to the energy of the non-interacting hadrons. Such an energy shift ΔE can be translated into the scattering phase shift at low energies and hence to the s -wave scattering length in the limit of zero relative momentum. Applications of Lüscher's formula to numerical simulations in lattice QCD have been previously done for π - π , π - N and N - N systems in Refs. [19, 20, 21, 22, 23] and also for a hypothetical bound state system in Ref. [24]. Our lattice data show that the low-energy interaction of the charmonia with light hadrons is always attractive. Among others, the charmonium- π interaction is quite small in accordance with the current algebra result, while the charmonium- ρ and charmonium- N interactions are likely to be large and may even support the charmonium-nucleus bound states according to the phenomenological analyses mentioned above.

This paper is organized as follows. In Sec. II, we recapitulate the method to calculate the s -wave scattering phase shift in lattice QCD and discuss its application of the Lüscher's phase-shift formula to the case of attractive interactions. In Sec. III, details of our Monte Carlo simulations and numerical results of J/ψ -hadron and η_c -hadron interactions at low energy are given. Physical implications of our results are also discussed. Finally, Sec. IV is devoted to summary and concluding remarks. In Appendix A, some details of the spin projections for J/ψ - ρ and J/ψ - N systems are described.

II. TWO HADRONS IN A FINITE BOX

It has been shown by Lüscher that the s -wave scattering phase shift is related to the energy shift ΔE in the total energy of two hadrons in a finite box [18]. To measure the total energy of two hadrons (h_1 and h_2) in the center-of-mass frame, we define the following four-point correlation function:

$$G^{h_1-h_2}(t_4, t_3; t_2, t_1) = \left\langle \mathcal{O}^{h_2}(t_4) \mathcal{O}^{h_1}(t_3) (\mathcal{O}^{h_2}(t_2) \mathcal{O}^{h_1}(t_1))^\dagger \right\rangle, \quad (2)$$

where each hadron is projected onto the zero momentum state by the summation over all spatial coordinates \vec{x} , i.e. $\mathcal{O}^h(t) = \sum_{\vec{x}} \mathcal{O}^h(\vec{x}, t)$. To avoid the Fierz re-arrangement of two-hadron operators, we choose $t_4 = t_3 + 1$ and $t_2 = t_1 + 1$. Let us first consider here the scattering processes, J/ψ - π , J/ψ - ρ and J/ψ - N (Cases for η_c - π , η_c - ρ and η_c - N will be discussed in Sec. III G). Accordingly, the four-point correlation functions are defined by

$$G_{ij}^{J/\psi-\pi}(t, t_{\text{src}}) = \left\langle \mathcal{O}^\pi(t+1) \mathcal{O}_i^{J/\psi}(t) (\mathcal{O}^\pi(t_{\text{src}}+1) \mathcal{O}_j^{J/\psi}(t_{\text{src}}))^\dagger \right\rangle, \quad (3)$$

$$G_{ij;kl}^{J/\psi-\rho}(t, t_{\text{src}}) = \left\langle \mathcal{O}_i^\rho(t+1) \mathcal{O}_j^{J/\psi}(t) (\mathcal{O}_k^\rho(t_{\text{src}}+1) \mathcal{O}_l^{J/\psi}(t_{\text{src}}))^\dagger \right\rangle, \quad (4)$$

$$G_{ij}^{J/\psi-N}(t, t_{\text{src}}) = \left\langle \mathcal{O}^N(t+1) \mathcal{O}_i^{J/\psi}(t) (\mathcal{O}^N(t_{\text{src}}+1) \mathcal{O}_j^{J/\psi}(t_{\text{src}}))^\dagger \right\rangle. \quad (5)$$

Here we use the conventional interpolating operators,

$$\mathcal{O}_\mu^{J/\psi}(\vec{x}, t) = \bar{c}_a(\vec{x}, t) \gamma_\mu c_a(\vec{x}, t), \quad (6)$$

$$\mathcal{O}^\pi(\vec{x}, t) = \bar{u}_a(\vec{x}, t) \gamma_5 d_a(\vec{x}, t), \quad (7)$$

$$\mathcal{O}_\mu^\rho(\vec{x}, t) = \bar{u}_a(\vec{x}, t) \gamma_\mu d_a(\vec{x}, t), \quad (8)$$

$$\mathcal{O}^N(\vec{x}, t) = \epsilon_{abc} [u_a^T(\vec{x}, t) C \gamma_5 d_b(\vec{x}, t)] u_c(\vec{x}, t), \quad (9)$$

for J/ψ , π , ρ and N , respectively. C is the charge conjugation matrix, $C = \gamma_4 \gamma_2$. Also, a , b and c are color indices, i , j , k and l are spatial Lorentz indices, and u , d and c are the up, down and charm quark fields. For the s -wave J/ψ - π scattering, the total spin is restricted to be 1. Then we simply choose diagonal correlation averaged over the spatial indices, $\frac{1}{3} \sum_i G_{ii}^{J/\psi-\pi}(t, t_{\text{src}})$, to extract the scattering length. On the other hand, for s -wave J/ψ - ρ and J/ψ - N scatterings, different total spin states are allowed: Spin-0, 1 and 2 states for J/ψ - ρ and spin-1/2 and 3/2 states for J/ψ - N . Therefore, we need appropriate spin projections to disentangle each spin contribution from four-point correlation functions. Details of such spin projection are described in Appendix A.

The hadronic two-point functions are defined as $G_h(t, t_{\text{src}}) = \langle \mathcal{O}^h(t) \mathcal{O}^{h\dagger}(t_{\text{src}}) \rangle$. For the vector mesons such as J/ψ and ρ , we take an average over the spatial Lorentz indices as $\frac{1}{3} \sum_{i=1,2,3} \langle \mathcal{O}_i^h(t) \mathcal{O}_i^{h\dagger}(t_{\text{src}}) \rangle$ so as to obtain possible reduction of statistical errors. Note that we have neglected the disconnected diagrams (such as self-annihilation of J/ψ) in evaluating the two-point function of J/ψ and the four-point functions with J/ψ in our simulations. Contributions from the disconnected diagrams in the vector channel are known to be negligibly small for strange and charm quarks in numerical simulations [25, 26] in accordance with the mechanism of OZI suppression.

Let us now define a ratio $R_{J/\psi-h}(t)$ to extract the total energy of two hadrons ($E_{J/\psi-h}$) relative to the total energy of individual hadron ($M_{J/\psi}$ and M_h):

$$R_{J/\psi-h}(t) = \frac{G_{J/\psi-h}(t, t_{\text{src}})}{G_{J/\psi}(t, t_{\text{src}})G_h(t+1, t_{\text{src}}+1)} \xrightarrow{t \gg t_{\text{src}}} \exp(-\Delta E \cdot t), \quad (10)$$

where

$$\Delta E = E_{J/\psi-h} - (M_{J/\psi} + M_h). \quad (11)$$

Assuming that two hadrons do not form a bound state, we can introduce their relative momentum k outside the interaction range through

$$\sqrt{M_{J/\psi}^2 + k^2} + \sqrt{M_h^2 + k^2} = E_{J/\psi-h}, \quad (12)$$

where k should vanish as $1/L$ with increasing L if there is no bound state in this channel.

Assuming that the interaction range R is smaller than a half of the lattice size, $R < L/2$, the s -wave phase shift in a finite box, $\delta_0(k)$, may be written as [18]

$$\frac{2\mathcal{Z}_{00}(1, q)}{L\pi^{1/2}} = k \cot \delta_0(k) = \frac{1}{a_0} + O(k^2), \quad (13)$$

where $q (\equiv (\frac{kL}{2\pi})^2)$ takes a non-integer value due to the two-particle interaction. The function $\mathcal{Z}_{00}(1, q)$ is an analytic continuation of the generalized zeta function, $\mathcal{Z}_{00}(s, q) \equiv \frac{1}{\sqrt{4\pi}} \sum_{\mathbf{n} \in \mathbf{Z}^3} (\mathbf{n}^2 - q)^{-s}$, from the region $s > 3/2$ to $s = 1$. The s -wave scattering length a_0 is defined through the small k limit of the above formula.

If a_0/L is sufficiently small, then one can make a Taylor expansion of the phase-shift formula (13) around $q^2 = 0$ and obtain [18]

$$\Delta E = -\frac{2\pi a_0}{\mu L^3} \left(1 + c_1 \frac{a_0}{L} + c_2 \left(\frac{a_0}{L} \right)^2 \right) + O(L^6) \quad (14)$$

with $c_1 = -2.837297$ and $c_2 = 6.375183$. μ denotes the reduced mass of two hadrons, $\mu = M_{J/\psi}M_h/(M_{J/\psi} + M_h)$. For $\Delta E > 0$, Eq. (14) with an expansion up to $O(L^{-4})$ and that up to $O(L^{-5})$ have a real and negative solution for a_0 . On the other hand, for $\Delta E < 0$, the expansion up to $O(L^{-4})$ gives no real solution for

$$\Delta E < -\frac{\pi}{2|c_1|\mu L^2}, \quad (15)$$

although the expansion up to $O(L^{-5})$ always has a real solution. Therefore, we can use Eq. (15) as a necessary condition to test the convergence of the large- L expansion. If this condition is not satisfied or marginally satisfied, we need to use the full expression of (13) to extract a_0 from ΔE . Eqs. (13-15) are the basic formulas to be utilized in the following sections.

III. NUMERICAL RESULTS AND DISCUSSIONS

We have performed simulations in quenched QCD with the single plaquette gauge action

$$S_g = \beta \sum_p \left\{ 1 - \frac{1}{3} \text{Re}[\text{Tr}U_p] \right\}, \quad (16)$$

where $\beta = 6/g^2$, $U_p = U_{\mu\nu}(n)$ and $\sum_p = \sum_n \sum_{\mu<\nu}$, and the Wilson fermion action

$$S_f = \sum_{n,m} \bar{q}(n) \left\{ \delta_{n,m} - \kappa \sum_{\mu} \left[(1 - \gamma_{\mu}) U_{\mu}(n) \delta_{n+\mu,m} + (1 + \gamma_{\mu}) U_{\mu}^{\dagger}(m) \delta_{n-\mu,m} \right] \right\} q(m), \quad (17)$$

where κ is the hopping parameter defined as $\kappa = \frac{1}{2(am_q+4)}$ with the lattice spacing a and quark mass m_q . We generate gauge ensembles at a fixed gauge coupling $\beta = 6/g^2 = 6.2$ with three different lattice sizes, $L^3 \times T = 24^3 \times 48$, $32^3 \times 48$ and $48^3 \times 48$. According to the Sommer scale [27, 28], $\beta = 6.2$ in the quenched approximation corresponds to a lattice cutoff of $a^{-1} \simeq 2.9$ GeV, which may be marginal to handle low-lying $c\bar{c}$ mesons on the lattice. We compute the quark propagators at three values of the hopping parameter $\kappa = \{0.1520, 0.1506, 0.1489\}$, which correspond to $M_{\pi}/M_{\rho} = 0.68, 0.83, 0.90$. $\kappa_c = 0.1360$ is reserved for the charm-quark mass. Simulation parameters and the number of the gauge samples are summarized in Table I. Preliminary accounts for $L=24$ and 32 cases are given in Ref. [29].

For the update algorithm, we adopt the Metropolis algorithm with 20 hits at each link update. The first 10000 sweeps are discarded for thermalization. The gauge ensembles in each simulation are separated by 1200 ($L=48$), 800 ($L=32$) and 600 ($L=24$) sweeps. For the matrix inversion, we use BiCGStab algorithm and adopt the convergence condition $|r| < 10^{-8}$ for the residues. We calculate smear-point quark propagators with a box-type smeared source which are located at $t_{\text{src}} = 6$ for the light quarks and at $t_{\text{src}} = 5$ for the charm quark. To enhance the coupling to ground states of hadrons, we choose a 24^3 box source, of which spatial lattice size is about 1.6 fm, on all three volumes, instead of a wall (L^3 box). Since the box-type smeared source is gauge variant, Coulomb gauge fixing is carried out by a combination of an $SU(2)$ subgroup method and an overrelaxed steepest descent method. Details of this procedure may be found in Ref. [30]. To perform the precise parity projection for the nucleon, we adopt a procedure to take an average of two quark propagators which are subject to periodic and antiperiodic boundary conditions in time as described in Refs. [31, 32].

A. Energy shift ΔE

Hadron masses computed with the conventional single exponential fit are summarized in Table II. $\kappa_c = 0.1360$ reproduces the mass of $J/\psi(3097)$ approximately. The mass of pseudoscalar meson becomes $M_{\pi} \approx 0.6$ GeV for $\kappa = 0.1520$, 0.9 GeV for $\kappa = 0.1506$ and 1.2 GeV for $\kappa = 0.1489$ in our simulations.

The energy shifts of two-hadron systems ($J/\psi\pi$, $J/\psi\rho$ and $J/\psi N$) are determined by the large- t behavior of the ratio $R_{J/\psi-h}$ defined in Eq. (10). To find appropriate temporal windows for fitting, we define the effective energy shift by

$$\Delta E_{\text{eff}}(t) = \ln \frac{R_{J/\psi-h}(t)}{R_{J/\psi-h}(t+1)}, \quad (18)$$

which should show a plateau for large Euclidean time ($t \gg t_{\text{src}}$) and approaches to the true energy shift ΔE , if the statistics is sufficiently large.

As typical examples of our simulations, in Fig. 1 we show the effective mass $\Delta E_{\text{eff}}(t)$ as a function of t for $L = 24$ (top panels), 32 (middle panels) and 48 (bottom panels) at $\kappa = 0.1506$. In the figure, the left panels are for the $J/\psi\pi$ channel, the middle ones for the spin-0 $J/\psi\rho$ channel, and the right ones for the spin-1/2 $J/\psi N$ channel. Statistical uncertainty of $\Delta E_{\text{eff}}(t)$ is estimated by a single elimination jack-knife method.

As seen from this figure, the effective energy shift is quite small compared to the mass of each hadron. Nevertheless, strong correlation between the numerator and denominator in the ratio $R_{J/\psi-h}$ can help to expose such a tiny shift. An important observation is that the negative energy shift is found in all channels of Fig. 1, which implies that there exist attractive interactions between J/ψ and light hadrons (π , ρ and N).

One should, however, notice that the signals become quite noisy for t far away from the sources at $t_{\text{src}} = 5$ and 6 . Therefore, we need to make appropriate choice of the fitting window in $[t_{\text{min}}, t_{\text{max}}]$ to extract ΔE from the data. Since the two-point correlation functions are well dominated by ground state hadrons (J/ψ , π , ρ and N) for $t > 20$, a reasonable choice of the lower bound is $t_{\text{min}} \sim 20$. The upper bound may be chosen so that we have a reasonable value of χ^2/dof in the fitting interval. Three horizontal solid lines in each panel of Fig. 1 represent the fitting range thus determined together with the value of ΔE and its 1σ deviation obtained by a covariant single exponential fit to the ratio $R_{J/\psi-h}$. The fitting range is chosen to be the same for the data with equal L . The results of energy shift obtained in the above procedure are summarized in Tables III, IV and V.

B. Quark mass dependence of the energy shifts

Fig. 2 shows the quark mass dependences of the energy shift ΔE for $L = 24$ (upper panels), $L = 32$ (middle panels) and $L = 48$ (lower panels). The left panels are for the $J/\psi\pi$ channel, the middle ones for the spin-0 $J/\psi\rho$ channel and the left ones for the spin-1/2 $J/\psi N$ channel. Open circles show the results evaluated at three values of the hopping parameter for the light hadrons, $\kappa = 0.1520, 0.1506$ and 0.1489 . We do not find appreciable spin dependence of the energy shift within the error bars in the $J/\psi\rho$ and $J/\psi N$ channels.

The $J/\psi\pi$ channel has a special feature in the sense that the low-energy pion decouples from any hadrons in the chiral limit as discussed in Sec. 1. In other words, ΔE of the $J/\psi\pi$ system should vanish in simultaneous chiral and infinite volume limits. The top, middle and bottom panels for the $J/\psi\pi$ channel in Fig. 2 indeed suggest such a tendency. This will be quantified later in Sec. III D.

To make an extrapolation of ΔE to the chiral limit, we adopt a simple formula:

$$a\Delta E = c + c'(aM_\pi)^2, \quad (19)$$

where c and c' are determined numerically from the data. In Fig. 2, full circles represent the energy shifts linearly extrapolated by Eq. (19) with the physical pion mass squared ($M_\pi = 140$ MeV). For the $J/\psi\rho$ and $J/\psi N$ channels, we show also the results (full squares) obtained from the weighted average of the data for two heavy-quark masses ($\kappa = 0.1506$ and 0.1489). The purpose is to check the sensitivity from the lightest data points which have relatively large error bars. We find that results of full circles and squares are in agreement with each other within the errors, and hence we quote the results evaluated by Eq. (19) in the following sections.

C. Volume dependence of the energy shifts

In Fig. 3, we show the volume dependence of the energy shift ΔE at the physical point ($M_\pi = 140$ MeV). The left panel is for the $J/\psi\pi$ channel, the middle for the spin-0 $J/\psi\rho$ channel and the right for the spin-1/2 $J/\psi N$ channel. The horizontal axis denotes the spatial size L and the vertical axis the energy shift ΔE . The dashed lines indicate the lower boundary given in Eq. (15): If the data points come below the dashed lines, the $1/L$ -expansion of the phase-shift formula is no longer justified.

The volume dependence of the energy shift ΔE is a key quantity to discuss the validity of the large- L expansion of the phase-shift formula. We find that the absolute value of the energy shift in the $J/\psi\pi$ channel of Fig. 3 decreases monotonically from $L = 24$ to 48 , which is consistent with the leading $1/L^3$ behavior shown in Eq. (14). On the other hand, the energy shift in the $J/\psi\rho$ and $J/\psi N$ channels do not show such monotonic decrease due to rather small values of ΔE at $L = 24$. This implies that the lattice size $L = 24$ ($La \sim 1.6$ fm) is too small to satisfy the condition $L > 2R \sim 2a_0$ so that the convergence of the power series in Eq. (14) is questionable or even the phase-shift formula in Eq. (13) itself is invalid. Thus, in the $J/\psi\rho$ and $J/\psi N$ channels, we do not take the results of $L = 24$ as physical in the following analyses.

D. Volume dependence of scattering lengths

In the left panel of Fig. 4, we show the volume dependence of the s -wave scattering length $a_0^{J/\psi\pi}$ at the physical point ($M_\pi = 140$ MeV) obtained by applying the phase-shift formula (13) to ΔE in Fig. 3. The horizontal axis is the spatial size L and the vertical axis is the scattering length. By taking into account the error bars for $L = 48$ due to the limited statistics, we do not find appreciable L dependence for the $J/\psi\pi$ scattering lengths. Also, the scattering length is positive, which implies attraction between J/ψ and π at low energy.

In the middle panel of Fig. 4, we show the volume dependence of the s -wave scattering length $a_0^{J/\psi\rho}$ obtained by Eq. (13). Within the error bars, different spin states have similar scattering lengths. The statistics in the $L = 24$ case is much better than $L = 32$ and 48 . However, the $L = 24$ data is contaminated by significant finite size effect as discussed in Sec. III C on the basis of Fig. 3. The scattering lengths for $L = 32$ and 48 show the positive values.

In the right panel of Fig. 4, we show the volume dependence of the $J/\psi N$ scattering length $a_0^{J/\psi N}$ obtained by Eq. (13). Similar to the case in the $J/\psi\rho$ channel, we do not find appreciable spin dependence within the error bars. Here the same discussion as the $J/\psi\rho$ channel applies to the $L = 24$ data. Although we need to increase statistics to make definite conclusion, the scattering length in $J/\psi N$ channel for $L = 32$ and 48 is positive and is considerably larger than that in the $J/\psi\pi$ channel.

In Table VI, we summarize the *s*-wave scattering lengths in lattice units at the physical point ($M_\pi=140$ MeV) and at the chiral limit ($M_\pi = 0$). The table shows a clear tendency,

$$0 < a_0^{J/\psi-\pi} \ll a_0^{J/\psi-\rho} < a_0^{J/\psi-N}. \quad (20)$$

This indicates that (i) there is always attraction between J/ψ and light hadrons, and (ii) there may be some relation between the strength of the attraction and the light-hadron properties such as the spatial size of light hadrons, or the number of constituent quarks in the light hadrons. To clarify the point (ii) further, it will be necessary not only to make high statistics simulations but also to carry out systematic calculations for the interactions of J/ψ with various light hadrons. It is also worth mentioning here that the *s*-wave J/ψ - π scattering length obtained at each volume is consistent with zero in the chiral limit within 1 or 2 standard deviations. This is in accordance with the current algebra result discussed in Eq. (1).

E. Scattering lengths in the physical units

In Table VII, the results of the *s*-wave scattering lengths, $a_0^{J/\psi-h}$, for each h with different spin states are tabulated, where “SAV” implies the results after the spin average. We show the results of two different methods to extract the scattering length from the energy shift.

“PSF (=Phase Shift Formula)” implies the method by using the phase-shift formula in Eq. (13) without making the $1/L$ -expansion. This is what we utilized to extract the numbers in Table VI. In this case, the final results of the scattering lengths are obtained by an average over the scattering lengths obtained in different volumes. In an alternative method indicated by “LLE (=Leading large- L Expansion)” we take the leading $1/L$ formula in Eq. (14), $\Delta E(L) = A \cdot L^{-3}$, and calculate A by fitting the volume dependence of the energy shift. The scattering length is then extracted as $a_0^{J/\psi-h} = -\mu A/2\pi$. The values of A obtained through this method are summarized in Table VIII. Theoretically, PSF is more rigorous than LLE. Nevertheless, the latter is useful to estimate a systematic error caused by a finite L .

As we have discussed in Sections III C and III D, we know that $L = 24$ is not large enough to extract any useful information in the J/ψ - ρ and J/ψ - N channels. Therefore, in both PSF and LLE, we use only the data for $L = 32$ and 48 in the J/ψ - ρ and J/ψ - N channels, while we use all data ($L = 24, 32$ and 48) in the J/ψ - π channel.

As seen in Table VII, the results obtained from two analysis (PSF and LLE) agree with each other within the errors. Especially, in the J/ψ - π case, both estimates are fairly consistent with each other. The table also shows the elastic cross sections at the threshold given by $\sigma_{\text{el}} = 4\pi a_0^2$. We find that the *s*-wave scattering length in the J/ψ - π channel is quite small, 0.0119(39) fm, but definitely positive. Therefore, we conclude that the J/ψ - π interaction is attractive at least at low energy. The soft pion theorem, where implies that the pion should decouple from any other hadrons in the chiral limit ($M_\pi = 0$), is an account for such smallness of the *s*-wave scattering length. The J/ψ - π elastic cross section at the threshold is evaluated as $\sigma_{\text{el}}^{J/\psi-\pi} = 0.018^{+0.013}_{-0.010}$ mb. This is consistent with a phenomenological analysis based on short distant QCD by Fujii and Kharzeev [16].

Although statistical errors in J/ψ - ρ and J/ψ - N channels are quite large, we find that *s*-wave scattering lengths in these channels are likely to be positive and are at least an order of magnitude larger than the pion case. As for the J/ψ - N channel, the scattering length from QCD sum rules by Hayashigaki [12], gluonic van der Waals interaction by Brodsky *et al.* [4], and the QCD multipole expansion by Voloshin *et al.* [13] show that the *s*-wave scattering length is about 0.1 fm, 0.25 fm, and 0.37 fm or larger, respectively. Our central value of the scattering length 0.71 fm from PSF (0.39 fm from LLE) is comparable or even larger than those estimates, but we need to increase statistics of our data to draw solid comparison.

F. Possible contaminations from channel mixings

Before closing the discussion on J/ψ -hadron scattering lengths, we comment on possible contaminations from the η_c - h and $D\bar{D}$ states. If there were open channels with lower energy than the J/ψ -hadron system at the threshold, the Lüscher’s formula for extracting the scattering phase shift from ΔE in the desired channel is not applicable.

The J/ψ - π system is free from the contamination of the η_c - π subthreshold state. This is because the *s*-wave η_c - π state has different total spin from the *s*-wave J/ψ - π state. On the other hand, for the J/ψ - ρ case, we cannot exclude the possible contamination of the η_c - ρ state to the spin-1 J/ψ - ρ state and that of the $D\bar{D}$ state to the spin-0 J/ψ - ρ state. Only the highest spin state (spin-2) is definitely free from such contaminations. This is true also for the case of J/ψ - N system: The highest spin state (spin-3/2) is free from the contamination of the η_c - N state.

Thus, strictly speaking, the spin-1 $J/\psi\text{-}\pi$, the spin-2 $J/\psi\text{-}\rho$ and the spin-3/2 $J/\psi\text{-}N$ states are the safe channels in determining the s -wave scattering phase shifts from the Lüscher's formula, although in our simulations we do not find any appreciable difference among different spin channels within the error bars.

G. η_c -hadron interactions

The scattering length of η_c with light hadrons can be performed in exactly the same way as the J/ψ case by using the conventional η_c interpolating operator as in Sec. II:

$$\mathcal{O}^{\eta_c}(\vec{x}, t) = \bar{c}_a(\vec{x}, t)\gamma_5 c_a(\vec{x}, t). \quad (21)$$

In the present paper, we neglect the disconnected diagrams in both two-point function of η_c and the related four-point functions as we have done in the case of J/ψ . From the theoretical point of view, neglecting the disconnected diagrams in the η_c channel is less justified than that in the J/ψ channel. On the other hand, it is numerically observed that the contributions from the disconnected diagrams are negligibly small for the charm quark even in the pseudoscalar channel [25, 26].

In our simulations the mass difference between the J/ψ and η_c is about 30 MeV, which is considerably smaller than the experimental value, 116 MeV. It is known that the hyperfine splitting is sensitive to the quenched approximation and the leading discretization error of the Wilson fermion action [25, 26]. Therefore, the spin-dependent observables in our simulations should be taken with caution.

Under these reservations, the volume dependences of the energy shift and the scattering length are shown in Figs. 5 and 6, respectively. Qualitative features of the figures are similar to those in the J/ψ case: The energy shift is definitely negative in all three channels at $L = 32$ and 48 . Also, we find $0 < a_0^{\eta_c\text{-}\pi} \ll a_0^{\eta_c\text{-}\rho} < a_0^{\eta_c\text{-}N}$. In the $\eta_c\text{-}\rho$ and $\eta_c\text{-}N$ channels, considerable finite L effect may exist at $L = 24$. All analyses are made in the same way as the case of J/ψ . Table IX contains two types of the chirally extrapolated value of the s -wave scattering length in all channels for each volume. In Table X, we compare results obtained from two different analyses (PSF and LLE). The coefficients A in LLE are tabulated in Table XI.

The s -wave $\eta_c\text{-}\pi$ scattering length turns out to be 0.0113 ± 0.0035 fm and the corresponding elastic cross section at the threshold is $\sigma_{\text{el}}^{\eta_c\text{-}\pi} = 0.016^{+0.011}_{-0.008}$ mb, both of which are very close to the values in the $J/\psi\text{-}\pi$ channel. Although we have large error bars, the scattering lengths in the $\eta_c\text{-}\rho$ and $\eta_c\text{-}N$ channels are also comparable with those in the $J/\psi\text{-}\rho$ and $J/\psi\text{-}N$ channels.

IV. SUMMARY AND CONCLUDING REMARKS

In this paper, we have studied the interactions of J/ψ and η_c with light-hadrons at low energy in quenched lattice QCD simulations. We calculated the scattering lengths of $J/\psi\text{-}\pi, \rho, N$ and $\eta_c\text{-}\pi, \rho, N$ from the energy shifts ΔE of two hadrons in a finite periodic box L^3 by using the Lüscher's phase-shift formula. We employed the lattice spacing $a \simeq (2.9 \text{ GeV})^{-1}$, three light-quark masses $M_\pi/M_\rho \simeq 0.68, 0.83, 0.90$, and three lattice sizes $La \approx 1.6, 2.2$ and 3.2 fm. Their values were utilized to perform analyses on quark-mass and lattice-size dependences of the energy shifts and the scattering lengths.

We did not find appreciable quark-mass dependence of ΔE in all channels, while in the $J/\psi\text{-}\pi$ channel it turned out that there is a tendency that the energy shift approaches zero in simultaneous chiral and large-volume limits as indicated in the current algebra analysis.

As for the volume dependence of the energy shifts, the $1/L^3$ behavior, which is expected from the asymptotic expansion of the Lüscher's formula in terms of $1/L$, was seen in the $J/\psi\text{-}\pi$ and $\eta_c\text{-}\pi$ channels. On the other hand, in the $J/\psi\text{-}\rho, N$ and $\eta_c\text{-}\rho, N$ channels, the data at $L = 24$ do not follow the $1/L^3$ behavior. Indeed, $La = 1.6$ fm is not large enough to accommodate even a single hadron such as N [33].

On the basis of the above observation, we adopted the data for $L = 24, 32$ and 48 in the $J/\psi(\eta_c)\text{-}\pi$ channel and the data for $L = 32$ and 48 in the $J/\psi(\eta_c)\text{-}\rho$ and $J/\psi(\eta_c)\text{-}N$ channels. Then we applied the Lüscher's formula without $1/L$ -expansion (which we call PSF) and with $1/L$ -expansion (which we call LLE). The resultant s -wave scattering lengths obtained from ΔE show that (i) the interaction of charmonia with light hadrons is always attractive, (ii) the scattering lengths in the $J/\psi(\eta_c)\text{-}\pi$ channels are quite small compared to other channels as consistent with the soft-pion theorem, and (iii) the scattering lengths in the $J/\psi(\eta_c)\text{-}\rho$ and $J/\psi(\eta_c)\text{-}N$ channels are at least an order of magnitude larger than those in the $J/\psi(\eta_c)\text{-}\pi$ channels.

The s -wave $J/\psi\text{-}\pi$ ($\eta_c\text{-}\pi$) scattering length is determined as 0.0119 ± 0.0039 fm (0.0113 ± 0.0035 fm) and the corresponding elastic cross section at the threshold becomes $0.018^{+0.013}_{-0.010}$ mb ($0.016^{+0.011}_{-0.008}$ mb). On the other hand, the

J/ψ - N (η_c - N) spin-averaged scattering length is 0.71 ± 0.48 fm (0.70 ± 0.66 fm) which has still a large statistical errors. Nevertheless, our result in the J/ψ - N channel may be compared with estimates from QCD sum rules (~ 0.1 fm), from the gluonic van der Waals interaction (~ 0.25 fm) and from the QCD multipole expansion (~ 0.37 fm or larger).

To have more quantitative understanding of the scattering lengths, in particular, of their magnitudes and spin dependences, we need to accumulate more statistics. Since our data for the $J/\psi(\eta_c)$ - $\rho(N)$ channels indicate that the scattering length is rather large so that the large- L expansion is not fully justified even for $L = 32$ and 48 . Therefore, it is important to go to larger volume to reduce the systematic errors due to the finite volume. Simulations with dynamical quarks are also an important future direction to be explored for full knowledge of the charmonium interactions.

Acknowledgement

We acknowledge to K. Sasaki for beneficial discussions and helping us to develop codes of the gauge fixing. We thank for A. Nakamura and his collaborators for giving us a chance to use their open source codes (Lattice Tool Kit [34]). S.S. thanks D. Kharzeev and T. Yamazaki for fruitful discussions. This work was supported by the Supercomputer Projects No.110 (FY2004) and No.125 (FY2005) of High Energy Accelerator Research Organization (KEK). T.H. was supported in part by the Grants-in-Aid of the Japanese Ministry of Education, Culture, Sports, Science, and Technology (No. 15540254).

Appendix A: Spin projection

In the cases of the s -wave J/ψ - ρ and J/ψ - N scatterings, there are different spin states: Spin-0, 1 and 2 states for the J/ψ - ρ and spin-1/2 and 3/2 states for the J/ψ - N . Therefore, the appropriate spin projections are required to disentangle each spin contribution from four-point correlation functions.

For the J/ψ - ρ system, the four point function, Eq. (4), can be expressed by the orthogonal sum of spin-0, spin-1 and spin-2 components:

$$G_{ij;kl}^{J/\psi-\rho}(t) = G^0(t)\hat{P}_{ij;kl}^0 + G^1(t)\hat{P}_{ij;kl}^1 + G^2(t)\hat{P}_{ij;kl}^2 \quad (22)$$

with spin projection operators defined by

$$\hat{P}_{ij;kl}^0 = \frac{1}{3}\delta_{ij}\delta_{kl}, \quad (23)$$

$$\hat{P}_{ij;kl}^1 = \frac{1}{2}(\delta_{ik}\delta_{jl} - \delta_{il}\delta_{jk}), \quad (24)$$

$$\hat{P}_{ij;kl}^2 = \frac{1}{2}(\delta_{ik}\delta_{jl} + \delta_{il}\delta_{jk}) - \frac{1}{3}\delta_{ij}\delta_{kl}. \quad (25)$$

Respective spin-projected correlators are given as

$$G^0(t) = \frac{1}{3}\sum_{i,j=1}^3 G_{ii;jj}^{J/\psi-\rho}(t), \quad (26)$$

$$G^1(t) = \frac{1}{6}\sum_{i,j=1}^3 \left(G_{ij;ij}^{J/\psi-\rho}(t) - G_{ij;ji}^{J/\psi-\rho}(t) \right), \quad (27)$$

$$G^2(t) = \frac{1}{10}\sum_{i,j=1}^3 \left(G_{ij;ij}^{J/\psi-\rho}(t) + G_{ij;ji}^{J/\psi-\rho}(t) - \frac{2}{3}G_{ii;jj}^{J/\psi-\rho}(t) \right), \quad (28)$$

where indices i and j should be summed over all spatial directions.

The four point function for the J/ψ - N system, Eq. (5), can be also decomposed into spin-1/2 and spin-3/2 components as

$$G_{ij}^{J/\psi-N}(t) = G^{1/2}(t)\hat{P}_{ij}^{1/2} + G^{3/2}(t)\hat{P}_{ij}^{3/2}. \quad (29)$$

Here, spin projection operators for spin-1/2 and spin-3/2 are given by

$$\hat{P}_{ij}^{1/2} = \frac{1}{3}\gamma_i\gamma_j, \quad (30)$$

$$\hat{P}_{ij}^{3/2} = \delta_{ij} - \frac{1}{3}\gamma_i\gamma_j. \quad (31)$$

Then, each spin part can be projected out as

$$G^{1/2}(t) = \sum_{i,j=1}^3 \hat{P}_{ij}^{1/2} G_{ji}^{J/\psi-N}(t) = \frac{1}{3} \sum_{i,j=1}^3 \gamma_i\gamma_j G_{ji}^{J/\psi-N}(t), \quad (32)$$

$$G^{3/2}(t) = \frac{1}{2} \sum_{i,j=1}^3 \hat{P}_{ij}^{3/2} G_{ji}^{J/\psi-N}(t) = \frac{1}{2} \sum_{i=1}^3 G_{ii}^{J/\psi-N}(t) - \frac{1}{6} \sum_{i,j=1}^3 \gamma_i\gamma_j G_{ji}^{J/\psi-N}(t), \quad (33)$$

where indices i and j are also summed over all spatial directions. Recall that respective contributions $G^{1/2}(t)$ and $G^{3/2}(t)$ possess non-trivial Dirac structure. To extract the particle contribution, we need to take a trace with the projection operator $(1 + \gamma_4)/2$ [31].

[1] S. J. Brodsky, I. A. Schmidt and G. F. de Teramond, Phys. Rev. Lett. **64**, 1011 (1990).

[2] D. A. Wasson, Phys. Rev. Lett. **67**, 2237 (1991).

[3] M. E. Luke, A. V. Manohar and M. J. Savage, Phys. Lett. B **288**, 355 (1992).

[4] S. Brodsky and G. A. Miller, Phys. Lett. B**412**, 125 (1997).

[5] G. F. de Teramond, R. Espinoza and M. Ortega-Rodriguez, Phys. Rev. D **58**, 034012 (1998).

[6] A. Sibirtsev, K. Tsushima, K. Saito and A. W. Thomas, Phys. Lett. B**484**, 23 (2000).

[7] K. Redlich, H. Satz and G. M. Zinovjev, Eur. Phys. J. C **17**, 461 (2000).

[8] A. Sibirtsev, K. Tsushima and A. W. Thomas, Phys. Rev. C**63**, 044906 (2001).

[9] F. Klingl, S. S. Kim, S. H. Lee, P. Morath and W. Weise, Phys. Rev. Lett. **82**, 3396 (1999) [Erratum-ibid. **83**, 4224 (1999)].

[10] M. E. Peskin, Nucl. Phys. B **156**, 365 (1979); G. Bhanot and M. E. Peskin, Nucl. Phys. B **156**, 391 (1979).

[11] D. Kharzeev, “Selected Topics in Nonperturbative QCD”, edited by A. Di. Giacomo and D. Diakonov, IOS, 1996, nucl-th/9601029 and references therein.

[12] A. Hayashigaki, Prog. Theor. Phys. **101**, 923 (1999).

[13] A. Sibirtsev and M. B. Voloshin, Phys. Rev. D**71**, 076005 (2005).

[14] T. Song and S. H. Lee, Phys. Rev. D**72**, 034002 (2005).

[15] S. Weinberg, Phys. Rev. Lett. **17**, 616 (1966).

[16] H. Fujii and D. Kharzeev, Phys. Rev. D **60**, 114039 (1999).

[17] J. -W. Chen and M. Savage, Phys. Rev. D **57**, 2837 (1998).

[18] M. Lüscher, Commun. Math. Phys. **105**, 153 (1986); Nucl. Phys. B**354**, 531 (1991).

[19] M. Guagnelli, E. Marinari and G. Parisi, Phys. Lett. B **240**, 188 (1990).

[20] S. R. Sharpe, R. Gupta and G. W. Kilcup, Nucl. Phys. B **383**, 309 (1992).

[21] M. Fukugita *et al.*, Phys. Rev. D**52**, 3003 (1995).

[22] T. Yamazaki *et al.* [CP-PACS Collaboration], Phys. Rev. D**70**, 074513 (2004). S. Aoki *et al.* [CP-PACS Collaboration], Phys. Rev. D**71**, 094504 (2005).

[23] S. R. Beane, *et al.* [NPLQCD Collaboration], Phys. Rev. D **73**, 054503 (2006); hep-lat/0602010.

[24] S. Sasaki and T. Yamazaki, hep-lat/0510032; PoS **LAT2005**, 061 (2005).

[25] C. McNeile and C. Michael [UKQCD Collaboration], Phys. Rev. D **70**, 034506 (2004).

[26] P. de Forcrand *et al.* [QCD-TARO Collaboration], JHEP **0408**, 004 (2004).

[27] R. Sommer, Nucl. Phys. B **411**, 839 (1994).

[28] M. Guagnelli, R. Sommer and H. Wittig [ALPHA collaboration], Nucl. Phys. B **535**, 389 (1998); S. Necco and R. Sommer, Nucl. Phys. B **622**, 328 (2002).

[29] K. Yokokawa, S. Sasaki, A. Hayashigaki and T. Hatsuda, hep-lat/0509189, PoS **LAT2005**, 215 (2005).

[30] S. Aoki *et al.* [CP-PACS Collaboration], Phys. Rev. D **67**, 034503 (2003).

[31] S. Sasaki, T. Blum and S. Ohta, Phys. Rev. D **65**, 074503 (2002).

[32] K. Sasaki and S. Sasaki, Phys. Rev. D**72**, 034502 (2005).

[33] In Ref. [29], we had only results on $L = 24$ and $L = 32$ lattices. Therefore, we could not rule out possibility of bound state formation in J/ψ - N channels since the volume dependence from $L = 24$ to $L = 32$ has an opposite tendency against that of scattering states. The $L = 48$ data shown in the present paper could rule out this possibility.

[34] S. Choe, S. Muroya, A. Nakamura, C. Nonaka, T. Saito and F. Shoji, Nucl. Phys. Proc. Suppl. **106**, 1037 (2002).

TABLE I: Simulation parameters in this study. The Sommer parameter $r_0 = 0.5$ fm is used to fix the scale [27, 28].

β	a [fm]	a^{-1} [GeV]	Lattice size ($L^3 \times T$)	$\sim La$ [fm]	Statistics
6.2	0.06775	2.913	$24^3 \times 48$	1.6	161
			$32^3 \times 48$	2.2	169
			$48^3 \times 48$	3.2	53

TABLE II: Fitted masses of pseudoscalar, vector and nucleon states in lattice units. We perform a covariant single exponential fit to two-point functions of each hadron in respective fitting ranges. The vector-meson mass at $\kappa = 0.1360$ in the physical unit is close to the mass of $J/\psi(3097)$ and hence the value is reserved for a charm quark. Other three hopping parameters are for light quarks. The box-to-point quark propagators are used in the present study, while the point-to-point quark propagators are used in Ref. [32] with different gauge configurations. The hadron masses in two approaches agree well with each other.

$L^3 \times T$	Fitting range	κ	aM_π	aM_ρ	aM_N
$24^3 \times 48$	[22,31]	0.1360	1.017(1)	1.027(1)	1.584(2)
		0.1489	0.415(1)	0.461(2)	0.722(4)
		0.1506	0.314(2)	0.383(3)	0.589(5)
		0.1520	0.213(2)	0.322(6)	0.467(10)
$32^3 \times 48$	[25, 34]	0.1360	1.020(1)	1.030(1)	1.594(2)
		0.1489	0.416(1)	0.463(1)	0.723(4)
		0.1506	0.315(1)	0.383(2)	0.592(4)
		0.1520	0.213(1)	0.317(4)	0.473(8)
$48^3 \times 48$	[17,26]	0.1360	1.016(1)	1.026(1)	1.581(3)
		0.1489	0.415(1)	0.460(2)	0.719(4)
		0.1506	0.314(1)	0.380(2)	0.586(4)
		0.1520	0.212(1)	0.311(3)	0.465(5)

TABLE III: Energy shifts ΔE in all J/ψ - h channels on the lattice with $L = 24$. The energy shifts are obtained from the ratios $R_{J/\psi-h}$ by the single exponential fit. The fitting range is chosen to be $22 \leq t \leq 31$ for all channels so as to be the same as that employed for spectroscopy of single hadrons for $L = 24$. The labels “phys.” and “chiral” show the values extrapolated to the physical point ($M_\pi = 140$ MeV) and to the chiral limit, respectively, with the linear quark-mass dependence in Eq. (19).

κ	$a\Delta E_{J/\psi-\pi}$	$a\Delta E_{J/\psi-\rho}^0$	$a\Delta E_{J/\psi-\rho}^1$	$a\Delta E_{J/\psi-\rho}^2$	$a\Delta E_{J/\psi-N}^{1/2}$	$a\Delta E_{J/\psi-N}^{3/2}$
0.1489	-0.0013(4)	-0.0020(4)	-0.0016(4)	-0.0012(4)	-0.0028(9)	-0.0032(9)
0.1506	-0.0014(4)	-0.0016(6)	-0.0012(6)	-0.0007(6)	-0.0023(10)	-0.0028(11)
0.1520	-0.0016(5)	-0.0006(13)	0.0003(13)	0.00010(13)	-0.0016(16)	-0.0023(17)
phys.	-0.0016(5)	-0.0008(12)	0.0000(12)	0.0007(12)	-0.0014(17)	-0.0022(17)
chiral	-0.0016(5)	-0.0008(12)	0.0001(12)	0.0007(12)	-0.0014(17)	-0.0022(18)

TABLE IV: Energy shifts for all J/ψ - h channels on the lattice with $L = 32$. The fitting range is chosen to be $25 \leq t \leq 34$ for all channels. The labels are the same as in Table III.

κ	$a\Delta E_{J/\psi-\pi}$	$a\Delta E_{J/\psi-\rho}^0$	$a\Delta E_{J/\psi-\rho}^1$	$a\Delta E_{J/\psi-\rho}^2$	$a\Delta E_{J/\psi-N}^{1/2}$	$a\Delta E_{J/\psi-N}^{3/2}$
0.1489	-0.0010(3)	-0.0021(5)	-0.0019(5)	-0.0016(5)	-0.0032(15)	-0.0035(16)
0.1506	-0.0009(3)	-0.0023(6)	-0.0021(6)	-0.0017(6)	-0.0028(14)	-0.0033(16)
0.1520	-0.0008(3)	-0.0027(11)	-0.0023(11)	-0.0018(10)	-0.0029(19)	-0.0039(22)
phys.	-0.0007(3)	-0.0028(11)	-0.0024(10)	-0.0019(10)	-0.0027(19)	-0.0036(21)
chiral	-0.0007(3)	-0.0028(11)	-0.0024(10)	-0.0020(10)	-0.0027(19)	-0.0036(22)

TABLE V: Energy shifts for all J/ψ - h channels on the lattice with $L = 48$. The fitting range is chosen to be $17 \leq t \leq 26$ for all channels. The labels are the same as in Table III.

κ	$a\Delta E_{J/\psi-\pi}$	$a\Delta E_{J/\psi-\rho}^0$	$a\Delta E_{J/\psi-\rho}^1$	$a\Delta E_{J/\psi-\rho}^2$	$a\Delta E_{J/\psi-N}^{1/2}$	$a\Delta E_{J/\psi-N}^{3/2}$
0.1489	-0.0010(3)	-0.0015(4)	-0.0014(4)	-0.0013(4)	-0.0025(8)	-0.0026(8)
0.1506	-0.0008(2)	-0.0014(3)	-0.0013(3)	-0.0012(3)	-0.0020(6)	-0.0022(6)
0.1520	-0.0005(2)	-0.0011(3)	-0.0009(3)	-0.0009(3)	-0.0017(6)	-0.0018(6)
phys.	-0.0004(2)	-0.0010(4)	-0.0008(4)	-0.0008(4)	-0.0014(7)	-0.0015(7)
chiral	-0.0004(2)	-0.0010(4)	-0.0008(4)	-0.0008(4)	-0.0014(7)	-0.0015(7)

TABLE VI: Results of the chirally extrapolated values of s -wave scattering lengths in lattice units for all J/ψ - h channels. The labels are the same as in Table III.

$L^3 \times T$		$a_0^{J/\psi-\pi}$	$a_0^{J/\psi-\rho}$	$a_0^{J/\psi-N}$	
		spin-0	spin-1	spin-1/2	spin-3/2
$24^3 \times 48$	phys.	0.16(5)	0.38(62)	-0.03(56)	-0.34(53)
	chiral	-0.0029(18)	0.38(62)	-0.03(56)	-0.34(53)
$32^3 \times 48$	phys.	0.17(7)	4.4(2.4)	3.6(2.0)	2.8(1.7)
	chiral	-0.0013(10)	4.4(2.4)	3.6(2.0)	2.7(1.6)
$48^3 \times 48$	phys.	0.33(17)	5.1(2.4)	3.8(2.1)	3.6(2.1)
	chiral	-0.0014(15)	5.0(2.4)	3.7(2.0)	3.6(2.1)

TABLE VII: The s -wave scattering lengths of J/ψ -hadrons and the elastic cross sections at the threshold in the physical unit. For the J/ψ - π channel, the data for all three volumes of $L = 24, 32$ and 48 are used, while for the J/ψ - ρ and J/ψ - N channels, only the data for $L = 32$ and 48 are used. In the table, “PSF” and “LLE” stand for the Phase Shift Formula and Leading large- L Expansion, respectively. “SAV” stands for the spin-averaged value, $\frac{1}{9}[5(a_0)_2 + 3(a_0)_1 + (a_0)_0]$, for the J/ψ - ρ channel and $\frac{1}{3}[2(a_0)_{3/2} + (a_0)_{1/2}]$ for the J/ψ - N channel.

Channel	Spin	From PSF		From LLE	
		a_0 [fm]	σ_{el} [mb]	a_0 [fm]	σ_{el} [mb]
$J/\psi-\pi$	1	0.0119 ± 0.0039	$0.018^{+0.013}_{-0.010}$	0.0119 ± 0.0025	$0.018^{+0.008}_{-0.007}$
$J/\psi-\rho$	0	0.32 ± 0.12	$12.9^{+11.0}_{-7.6}$	0.23 ± 0.06	$6.6^{+4.2}_{-3.2}$
	1	0.25 ± 0.10	$7.9^{+7.3}_{-4.9}$	0.19 ± 0.06	$4.6^{+3.3}_{-2.4}$
	2	0.21 ± 0.09	$5.5^{+5.6}_{-3.7}$	0.17 ± 0.06	$3.5^{+3.8}_{-2.0}$
	SAV	0.23 ± 0.08	$6.8^{+8.1}_{-4.2}$	0.18 ± 0.05	$4.1^{+3.9}_{-2.1}$
$J/\psi-N$	1/2	0.57 ± 0.42	41^{+83}_{-38}	0.35 ± 0.15	15^{+15}_{-10}
	3/2	0.88 ± 0.63	96^{+188}_{-89}	0.43 ± 0.16	23^{+20}_{-14}
	SAV	0.71 ± 0.48	64^{+116}_{-57}	0.39 ± 0.14	20^{+16}_{-12}

TABLE VIII: Fitting parameter A as the coefficient of the leading term in the large- L expansion of the energy shift. For the J/ψ - π channel, we used all energy shifts at $L = 24, 32$ and 48 to extract the fitting parameter A . On the other hand, for the J/ψ - ρ and J/ψ - N channels, we excluded the energy shifts at $L = 24$ for evaluating the parameters A .

	$A_{J/\psi-\pi}$	$A_{J/\psi-\rho}^0$	$A_{J/\psi-\rho}^1$	$A_{J/\psi-\rho}^2$	$A_{J/\psi-N}^{1/2}$	$A_{J/\psi-N}^{3/2}$
phys.	-24(5)	-101(28)	-84(26)	-73(25)	-115(48)	-140(52)

TABLE IX: Results of the chiral extrapolated values of s -wave scattering lengths in lattice units for all η_c -hadron channels. The labels are the same as in Table III.

$L^3 \times T$		$a_0^{\eta_c-\pi}$	$a_0^{\eta_c-\rho}$	$a_0^{\eta_c-N}$
$24^3 \times 48$	phys.	0.15(5)	-0.25(48)	1.10(1.29)
	chiral	-0.0025(15)	-0.25(48)	1.09(1.28)
$32^3 \times 48$	phys.	0.15(5)	2.8(1.6)	8.8(9.2)
	chiral	-0.0013(9)	2.7(1.6)	8.7(9.0)
$48^3 \times 48$	phys.	0.33(17)	3.4(1.8)	12.4(10.5)
	chiral	-0.0014(14)	3.4(1.8)	12.2(10.2)

TABLE X: The s -wave scattering lengths of η_c -hadrons and the elastic cross sections at the threshold in the physical unit. For the $\eta_c-\pi$ channel, the data for all three volumes of $L = 24, 32$ and 48 are used, while for the $\eta_c-\rho$ and η_c-N channels, only the data for $L = 32$ and 48 are used. The labels are the same as in Table VII.

Channel	Spin	From PSF		From LLE	
		a_0 [fm]	σ_{el} [mb]	a_0 [fm]	σ_{el} [mb]
$\eta_c-\pi$	0	0.0113 ± 0.0035	$0.016^{+0.011}_{-0.008}$	0.0112 ± 0.0024	$0.016^{+0.008}_{-0.006}$
$\eta_c-\rho$	1	0.21 ± 0.11	$5.3^{+7.5}_{-4.3}$	0.16 ± 0.05	$3.4^{+2.5}_{-1.8}$
η_c-N	$1/2$	0.70 ± 0.66	62^{+172}_{-62}	0.39 ± 0.14	19^{+16}_{-11}

TABLE XI: Fitting parameter A as the coefficient of the leading term in the large- L expansion of the energy shift. For the $\eta_c-\pi$ channel, we use all energy shifts at $L = 24, 32$ and 48 to extract the fitting parameter A . On the other hand, for the $\eta_c-\rho$ and η_c-N channels, we exclude the energy shifts at $L = 24$ for evaluating the parameters A .

	$A_{\eta_c-\pi}$	$A_{\eta_c-\rho}$	A_{η_c-N}
phys.	-23(5)	-72(23)	-127(47)

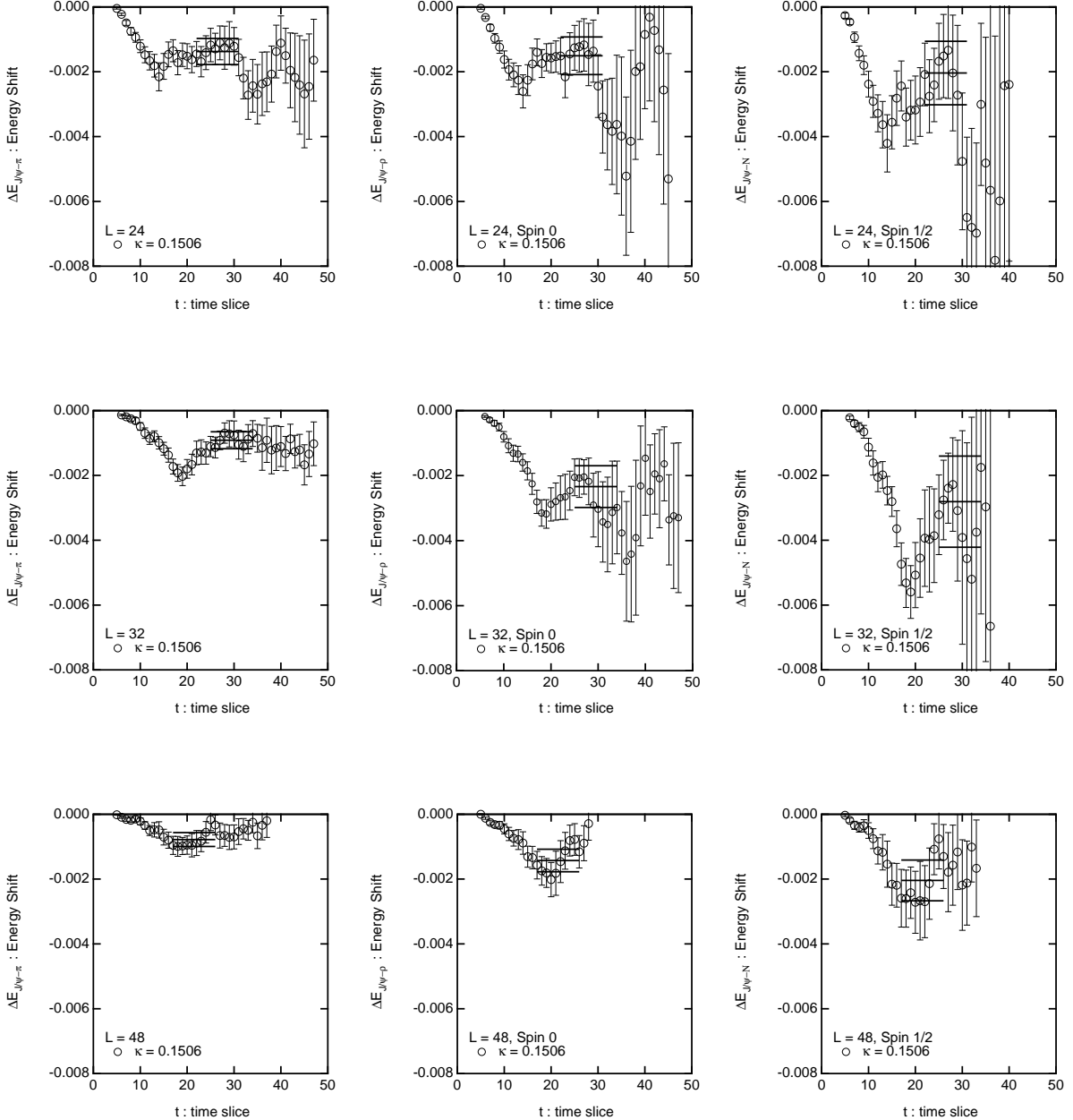


FIG. 1: The effective energy shifts ΔE in lattice units as a function of the time slice t . Hopping parameters of light hadrons and the J/ψ are fixed to be $\kappa = 0.1506$ and 0.1360 , respectively. Top (middle, bottom) panels are for $L = 24$ ($32, 48$). Left (middle, right) panels are for the $J/\psi\pi$ ($J/\psi\rho$ in spin-0, $J/\psi N$ in spin-1/2) channels. Source locations of light hadrons and the J/ψ are at $t_{\text{src}} = 6$ and 5 , respectively.

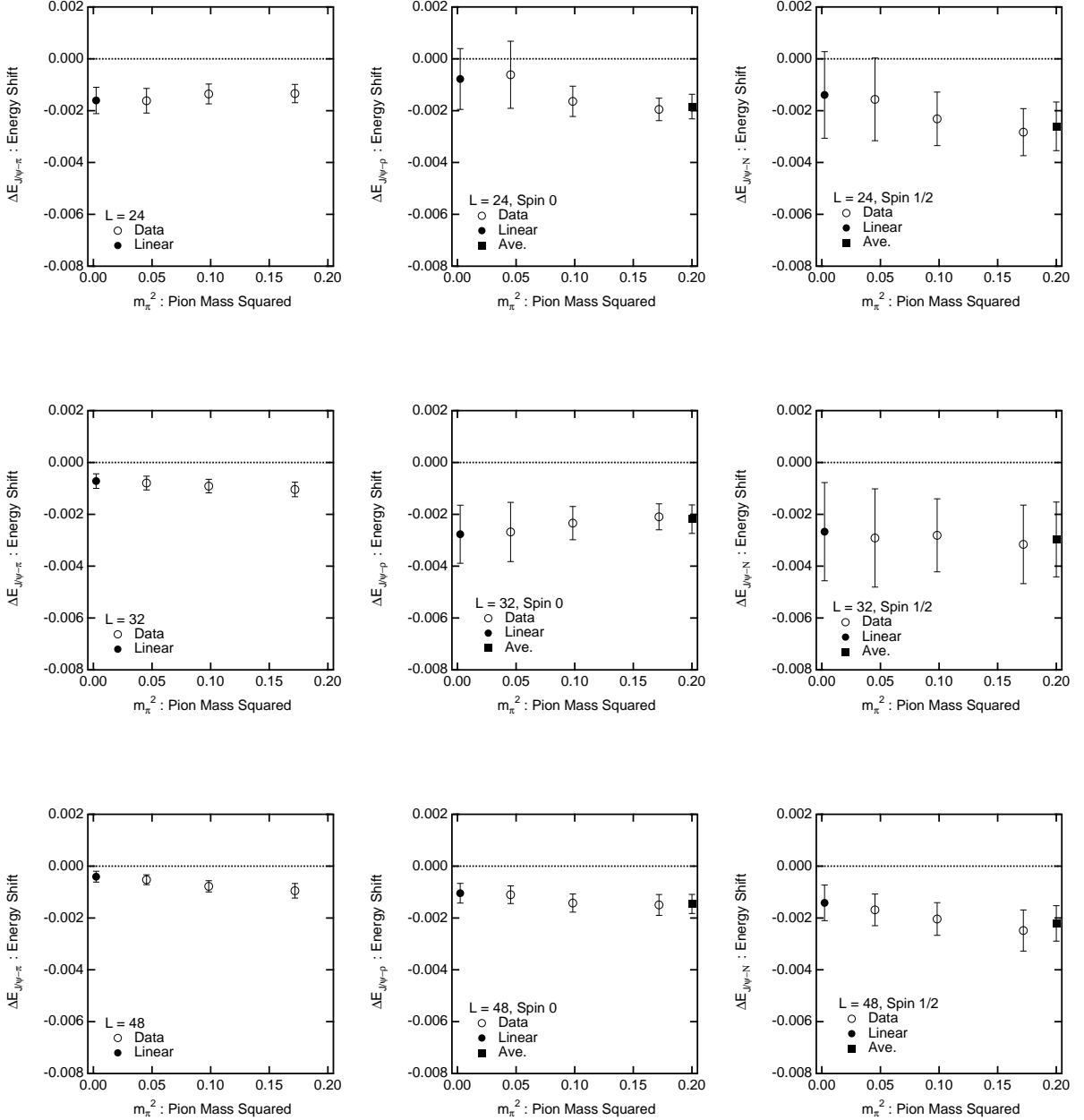


FIG. 2: The energy shifts ΔE as a function of the squared pion mass M_π^2 in lattice units. Upper (middle, lower) panels are for $L = 24$ (32, 48). Left (middle, right) panels are for the $J/\psi\text{-}\pi$ ($J/\psi\text{-}\rho$ in spin-0, $J/\psi\text{-}N$ in spin-1/2) channels. Open circles are the values fitted by the criterion obtained from the four-point function at the hopping parameters of light hadrons ($\kappa = 0.1489, 0.1506$ and 0.1520). Full circles are the values extrapolated to the physical point ($M_\pi = 140$ MeV) by using Eq. (19). Full squares are the values from weighted averages of heavy-quark results ($\kappa = 0.1489$ and 0.1506).

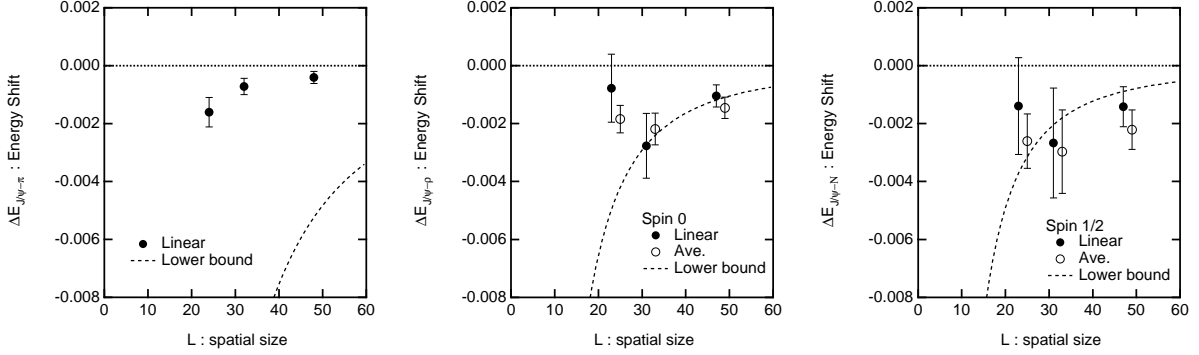


FIG. 3: The energy shifts ΔE as a function of spatial size L in lattice units. Left (middle, right) panel is for the $J/\psi\pi$ ($J/\psi\rho$ in spin-0, $J/\psi N$ in spin-1/2) channel. Full and open circles represent the values obtained from the linear chiral-extrapolation to the physical point, and the weighted average, respectively. The dashed curves show the lower boundary for the convergence of the large- L expansion of ΔE .

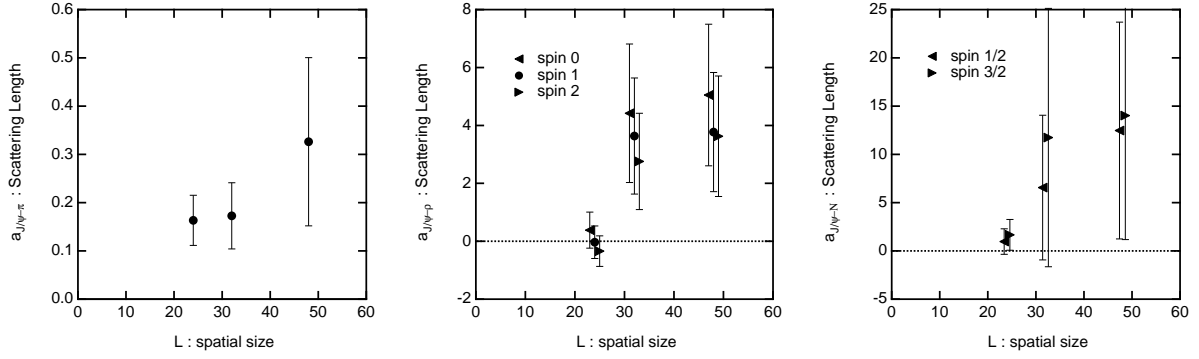


FIG. 4: The scattering lengths as a function of the spatial size L in lattice units for physical pion mass ($M_\pi = 140$ MeV). Left (middle, right) panel is for the $J/\psi\pi$ ($J/\psi\rho$, $J/\psi N$) channel.

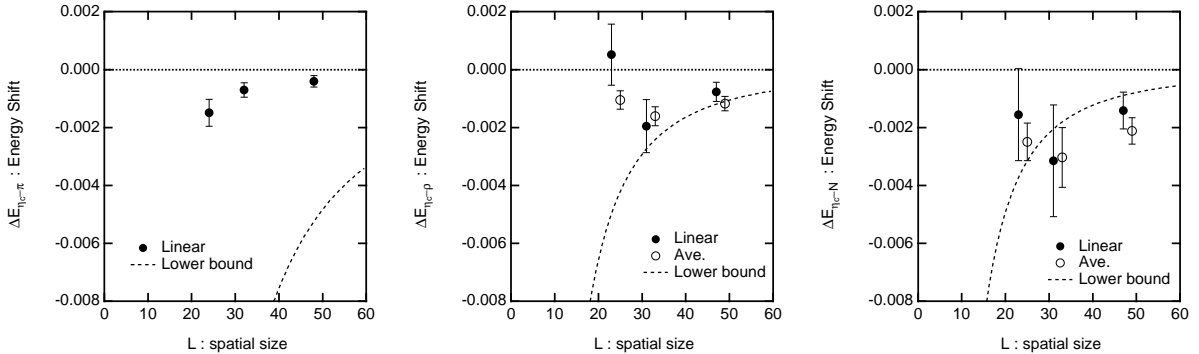


FIG. 5: The energy shifts ΔE as a function of spatial size L in lattice units. Left (middle, right) panel is for the $\eta_c\pi$ ($\eta_c\rho$, $\eta_c N$) channel. Full and open circles represent the values obtained from the linear chiral-extrapolation to the physical point, and the weighted average, respectively. The dashed curves show the lower boundary for the convergence of the large- L expansion of ΔE .

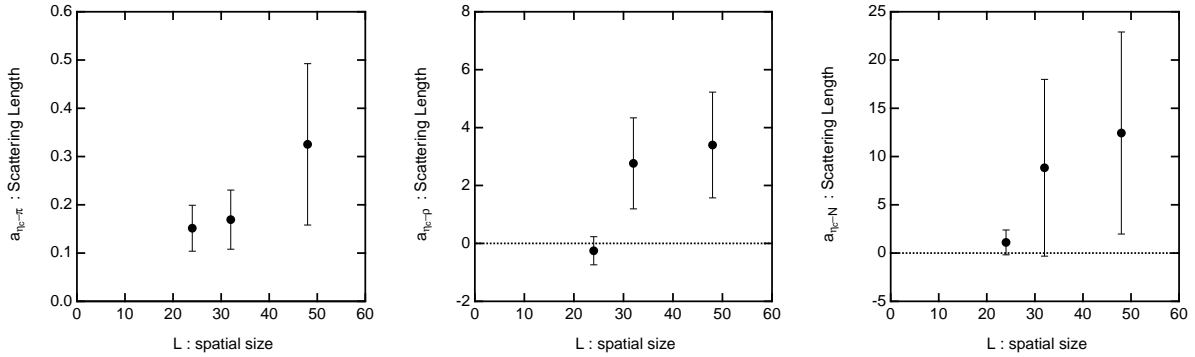


FIG. 6: The scattering lengths as a function of the spatial size L in lattice units for the physical pion mass ($M_\pi = 140$ MeV). Left (middle, right) panel is for the $\eta_c\text{-}\pi$ ($\eta_c\text{-}\rho$, $\eta_c\text{-}N$) channel.